

Article

Study of Breakdown Voltage Stability of Gas-Filled Surge Arresters in the Presence of Gamma Radiation [†]

Emilija Živanović * , Marija Živković and Sandra Veljković 

Faculty of Electronic Engineering, University of Niš, Aleksandra Medvedeva 14, 18000 Niš, Serbia

* Correspondence: emilija.zivanovic@elfak.ni.ac.rs

[†] This paper is an extended version of conference paper: Živković, M.; Dimitrijević, N.; Živanović, E. Statistical Analysis of Breakdown Voltage of Citel Gas-Filled Surge Arrester. In Proceedings of the 32nd International Conference on Microelectronics, Niš, Serbia, 12–14 September 2021; pp. 113–116.

Abstract: The results presented in this article relate to the study of the impact of gamma radiation on the breakdown voltage of gas-filled surge arrester manufactured by CITELE, Littelfuse and EPCOS at an operating voltage of 230 V. Radium was considered as a source of gamma radiation in this research. The stability of breakdown voltage as well as the reliability of gas-filled surge arresters of different manufacturers were investigated using different statistical methods. This gas component operation was based on processes that lead to electrical breakdown and discharge in gas. The breakdown voltage has a stochastic nature, and it is a subject of certain distribution. One thousand voltage measurements of breakdown voltage were carried out for each value of the voltage increase rate, from 1 V/s up to 10 V/s, with and without the presence of additional gamma radiation. The detailed statistical analysis of the obtained experimental data was performed for both cases for all three GFSA types. Moreover, the cumulative distribution functions of breakdown voltage were presented with the applied Weibull distribution fit. The coefficient of correlation as well as Pearson χ^2 test showed the strength of the relationship between the experimental distribution functions and the Weibull distribution fits. The values of the Weibull distribution coefficients for all voltage increase rates and for all components were also analyzed with and without gamma radiation.

Keywords: gas-filled surge arresters; stability; breakdown voltage; voltage increase rate; Weibull distribution function; gamma radiation



Citation: Živanović, E.; Živković, M.; Veljković, S. Study of Breakdown Voltage Stability of Gas-Filled Surge Arresters in the Presence of Gamma Radiation. *Electronics* **2022**, *11*, 2447. <https://doi.org/10.3390/electronics11152447>

Academic Editors: Padmanabhan Balasubramanian and Lidia Dobrescu

Received: 7 July 2022

Accepted: 19 July 2022

Published: 5 August 2022

Publisher's Note: MDPI stays neutral with regard to jurisdictional claims in published maps and institutional affiliations.



Copyright: © 2022 by the authors. Licensee MDPI, Basel, Switzerland. This article is an open access article distributed under the terms and conditions of the Creative Commons Attribution (CC BY) license (<https://creativecommons.org/licenses/by/4.0/>).

1. Introduction

As an important protection device, gas-filled surge arresters (GFSA as the acronym used in this article) can be used for transient overvoltage protection of electronic equipment. The breakdown voltage of GFSA usually deviates after long-term use and multiple discharges, which affects its stability and reliability. In order to study the reliability of CITELE 230 V GFSA [1], we performed a statistical analysis of breakdown voltage. However, in this paper, research was continued with the aim to investigate the breakdown voltage stability under the influence of gamma radiation in order to enable its further efficient application in various more complex electronic circuits for three different manufacturers.

In technology, overvoltage means that the potential of one point of a component or device in relation to another point or point of zero potential is greater than allowed. If the overvoltage is above a specific threshold, this might be a risk for the operators' safety as well as harmful to the devices themselves. Furthermore, exceeding the authorized levels of overvoltage can cause permanent or temporary damage to some electronic components and devices and also the occurrence of noise in transmission signals. Overvoltage can be caused by atmospheric discharges, electrostatic discharges, commutation overvoltage, radar pulses and electromagnetic pulses from a nuclear explosion. These types of discharges have a substantial impact on communications networks, causing component damage. The extreme type of overvoltage is atmospheric discharge because its occurrence is unpredictable.

Efficient overvoltage protection of systems and devices is very significant for their appropriate operation. Non-linear components utilized in overvoltage protection are gas-filled surge arresters. This component is also known in the literature as a surge voltage protector (SVP) or a gas discharge tube (GDT) [2–4]. One key disadvantage of GDTs is that they are used on low-power circuits because the follow current extinguishing capability is minimal. Switching type devices with considerable extinguishing capabilities are also available in the surge protection industry [5–7]. However, one key advantage is that switching type components provide a low I^2t stress to the equipment under protection [8]. GFSA operates on the principle of gas electrical breakdown. High stability (maximum allowable current up to 60 kA), wide range of protection levels (from 70 V to 1200 V), low intrinsic capacity (less than 1 pF) and low resistance in conducting regime (about 0.1 Ω) are some of the key advantages of implementing GFSA. It is worth noting that the breakdown process has a statistical nature, which is the reason why the breakdown voltage is not a fixed value. Between the time the higher voltage is applied and the time the current in GFSA begins to flow, there is a time gap. This parameter is the so-called delay response or the electrical breakdown delay time.

Components, which are most often used for protection against overvoltage, can be divided into linear and non-linear elements, according to the way of applying voltage at their ends when the current through them rises. Electric filters, whose most sensitive elements are capacitors, are linear elements for overvoltage protection. Non-linear overvoltage protection elements are more commonly utilized than linear ones, and they can be categorized into three classes based on manufacturing technology and operation principle. Transient suppresser diodes (TSDs), metal oxide varistors (MOVs) and gas-filled surge arresters (GFSAs) are examples of these devices. Various combined (hybrid) techniques are occasionally used to protect against overvoltage [2].

The most common GFSA nowadays is made up of two or three gaseous isolated electrodes contained in a ceramic or glass enclosure [2]. The electrodes are separated by millimeters or fractions of millimeters, and a homogenous electric field is created by them. The first electrode is connected with an overvoltage protected point, and the other is at zero potential. As a result of the low capacitance value, when the potential difference between the GFSA electrodes is less than the nominal value (DC breakdown voltage), the arrester has an infinite resistance, and capacitance does not impact the protected component. Electrical breakdown occurs in the interelectrode distance when the potential difference between the electrodes exceeds the nominal value due to the overvoltage, and the overvoltage is carried to the ground. As a result, the overvoltage wave is prevented from reaching the protected component, which is significant, given the trend of downsizing and increasing environmental electromagnetic contamination. To avoid edge effects, GFSA electrodes are commonly fabricated in the Rogowski cloud [9]. The electrodes are often composed of tungsten, which has a good melting temperature and thermal conductivity ratio. At pressures ranging from 100 Pa to 70 kPa, noble gases, such as argon, neon, krypton or xenon, or their mixtures are utilized as the insulating medium in GFSA. The chamber holding the electrodes and the noble gas must be well sealed, since noble gases are monoatomic and can quickly diffuse out of the chamber, especially when they are under compression. The working point is determined by the product of pressure and an interelectrode distance, which is on the abscissa, and the nominal voltage, which is the DC breakdown voltage on the ordinate, because the law of similarity is unmistakably valid for such setup [10,11]. On the Paschen's curve, the GFSA working point is around the Paschen's minimum. It is frequently found to the right of the minimum, where a streamer mechanism has caused the breakdown. It has recently been proposed that the GFSA working point be set at positions to the left of the minimum where an abnormal Paschen's mechanism causes the breakdown. This second option ensures greater working point stability over a longer length of time [12]. Similar investigation was conducted in nitrogen-filled gas tube, as could be seen for example in Refs. [13,14]. It should be noted that similar research with gaseous components was conducted, for example, with HVDC components estimating

the distribution of the electric field and the voltage holding of the designed geometry [15]. Ref. [15] also describes the research that concerns the correct modeling approach suitable to study high-voltage components in DC. Moreover, the investigations of the implementation and design of real-time breakdown voltage and temperature monitored system for single avalanche diodes are published in Ref. [16]. This is another example of the importance of studying breakdown voltage.

From numerous research works of different groups of authors, one can see the great importance of examining the influence of gamma radiation on the operation of different types of gas and semiconductor components. Among the others, in Refs. [17–19], the effects induced by previous irradiation and the total dose received strongly affect the subsequent stresses. Specifically, in the case of low-dose irradiation, following stress caused by working in specific applications, this appears to result in device degradation in the future. On the other hand, in the case of devices that previously have been exposed to higher doses of radiation, this effect is beneficial because it effectively anneals a portion of the radiation-induced degradation. In addition, Ref. [20] has shown that changes in the structures of GaN HEMTs occur during irradiation. As for gas-filled arresters [21], it has been established that the pre-breakdown current increased in the presence of gamma radiation and that the response time of GFSA was improved.

As previous research was related to the reliability test of GFSA [22,23], and the influence of radiation was examined through the behavior of memory curves in a gas-filled tube, as well as breakdown voltage, the aim of this paper is to investigate the influence of gamma radiation on the breakdown voltage stability of gas-filled surge arrester.

The basic statistical analysis was published in Ref. [1], and the previous effect of radiation on this type of gas arrester was reflected in the examination of memory curves [24] as well as the pre-breakdown current in relation to the applied voltage [25].

The paper is conceived in several sections. After introductory considerations of over-voltage and protection of electronic circuits from it and wide application of gas-filled arresters, a description of the GFSA sample as well as the source of radiation used in the experiment follows. The determination of the static breakdown voltage was performed using a discretized dynamic approach. In the Results and Discussion section, a graphical presentation of the basic statistical values for each voltage increase rate is given for irradiated components, with each set of measured data having a thousand measurements. Moreover, the frequency count of dynamic breakdown voltage is presented for the GFSA CITEL manufacturer with and without the presence of a radium source for three increase voltage rates, and comparisons are made for all three GFSA on $k = 1$ V/s. Then, the cumulative distribution of the measured data for the first three increase voltage rates is given, the results of fitting Weibull distribution are presented, the distribution parameter is determined, and their comparison is made. All experimental procedures and statistical analyses of the obtained values of breakdown voltage in the presence of gamma radiation were performed for all GFSA used in the experiments.

2. Experimental Method

2.1. Experimental Used Component

The geometry of the used gas-filled surge arresters for all manufacturers is similar and is represented in Figure 1. The inter-electrode distance is close to 6 mm. The precise type of gas, which is present in it, is not available. However, the manufacturer states that GFSA is filled with some noble gas at a pressure below the atmospheric.

The CITEL GFSA [26] is manufactured to operate at a voltage of 230 V, and DC sparkover voltage is between 184 V and 276 V (this confirms the fact that DC spark voltage tolerance is $\pm 20\%$). The typical specifications of gas-filled surge arresters at room temperature are: the maximum capacitance is less than 1.5 pF; the arc voltage has the value of ~ 30 V. Additionally, the parameter known as the nominal impulse discharge current is 25 kA for CITEL GFSA. The Littelfuse GFSA [27] is manufactured to operate at a voltage of 230 V and, with its DC spark voltage tolerance of $\pm 20\%$, the DC sparkover voltage is

between 184 V and 276 V. In this case, the maximum capacitance is less than 1.5 pF; the arc voltage has the value of ~15 V. Additionally, the nominal impulse discharge current is 20 kA. Lastly, EPCOS GFSA [28] is operating at a voltage of 230 V, while its DC sparkover voltage is between 196 V and 264 V with the DC spark voltage tolerance of $\pm 15\%$. The maximum capacitance of this GFSA at room temperature is less than 1.5 pF; the arc voltage has the value of ~12 V, whereas the nominal impulse discharge current is 10 kA. For clarity, the basic parameters of the tested samples of GFSA are presented in Table 1 [26–28].

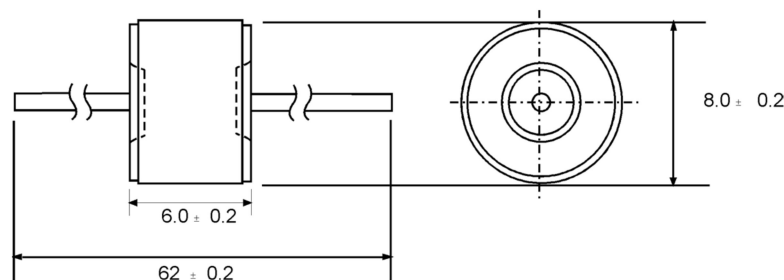


Figure 1. The geometry of gas-filled surge arrester.

Table 1. Gas-filled surge arresters' specifications at 25 °C.

Specifications of Gas-Filled Surge Arresters								
Component's Manufacturer	Operating Voltage AC (V)	Breakdown Voltage in the dc Mode (V)	DC Breakdown-Typical (V)	Insulation Resistance (GΩ)	Capacitance (pF)	Arc Voltage-on State Voltage (V)	Nominal Impulse Discharge Current (8/20 μs) (kA)	Impulse Sparkover Voltage (1.2/50 μs/6 kV)
CITEL	230	184 to 276	230	10	<0.8	~30	25	<900
Littelfuse	230	184 to 276	230	10	<1.5	~15	20	<700
EPCOS	230	196 to 264	230	10	<1.5	~12	10	<700

2.2. The Source of Gamma Radiation

Radium [29,30] is a silvery-white heavy metal that oxidizes rapidly when it is exposed to the air and has a density approximately half that of lead. Mostly, radium occurs naturally as radium-226, although several other isotopes exist. Only two radium isotopes—radium-226 and radium-228—have half-lives longer than a year. Radium-226 degrades slowly (half-life is about 1600 years) by producing alpha particles. Radium-226, which consists of 88 protons and 138 neutrons, is the only isotope of radium that is commercially available. Among others, the goal of this research is to investigate the contributions of gamma photons from $^{226}_{88}\text{Ra}$ radiation source and cosmic rays to the initiation of an electrical breakdown in commercially available, gas-filled surge arresters. The decay of radium-226 and its products generates dozens of distinct gamma rays with variable energy and yields; the energies range from less than 50 keV to around 2.5 MeV. The energy and numbers of gamma rays emitted by a source are dependent on how it is constructed, namely the sort of material utilized for the source encapsulation and its thickness. Generally, photons with energy less than roughly 50 keV are not significant from a dosage standpoint for the majority of realistic sealed sources of radium-226. If photons with energies less than 50 keV and also photons with yields greater than 1% are excluded, an effective gamma energy of approximately 0.74 MeV is obtained. This energy is calculated by multiplying each photon energy by its fractional yield, adding all such products and dividing by the sum of all photon yields. The source, which was used for irradiation in this experiment, has the activity $A \approx 12$ kBq. The formula $\dot{D}_e = AG/r^2$ was used in order to calculate the exposed dose rate \dot{D}_e . Here, r represents the distance between the source and electrode gap, and G is the gamma constant. The value of G is 1.7×10^{-18} C m² kg⁻¹ and r is 1 cm. Based on the formula, it was calculated that the value of the exposed dose rate was $\dot{D}_e \approx 2.04 \times 10^{-10}$ C kg⁻¹ s⁻¹.

2.3. Experimental Procedure

For the realization of the experiment, the system for measuring and data acquisition presented in detail in Refs. [23,31] was used. Figure 2 shows the equipment of the experiment:

- the computer, through which the parameters are set, activates the software and collects the data;
- DC high voltage source, step voltage generator and digital subsystem;
- source of radiation;
- gas-filled surge arrester.

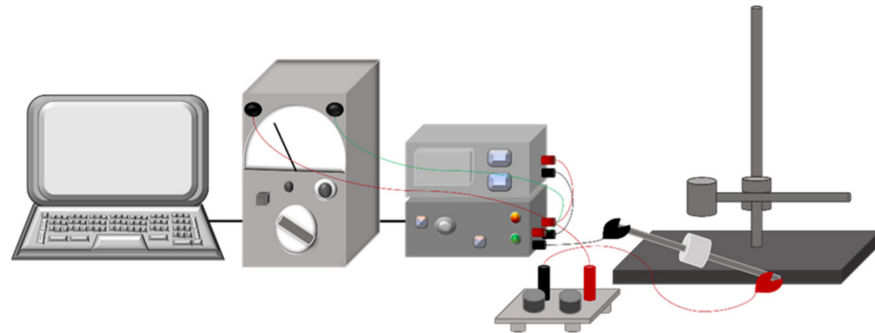


Figure 2. Graphical illustration of computer-controlled equipment of breakdown voltage measurement and data acquisition.

It can be emphasized that the system for breakdown voltage measurement consists of an analog and a digital subsystem. The analog subsystem consists of a DC high voltage source and step voltage generator, and their voltage difference applied to the gas-filled surge arrester. The step generator was designed as a voltage amplifier with $\times 100$ amplification. The digital subsystem contains a MICROCHIPs PIC18F2550 microcontroller and a D/A converter. The voltage from the D/A converters amplifies a hundred times and subtracts from the voltage of DC high voltage source output. The voltage at whose value the breakdown occurs is stored in the memory. After that, the gas-filled surge arrester is disconnected from the voltage for a predefined value of relaxation time τ . After this time, a new measurement starts, and this procedure continues for a thousand cycles at a predefined value of voltage increase rate.

In Figure 3, a schematic representation of the stepwise increase in the voltage to breakdown is shown. Here, U_p is the increasing voltage step, t_p is the duration of the step, t_g is the glow time, which is achieved by maintaining a constant value of the voltage U_g , U_k initial voltage, τ is the relaxation time, and U_{b1} , U_{b2} , ... are the values of the breakdown voltage.

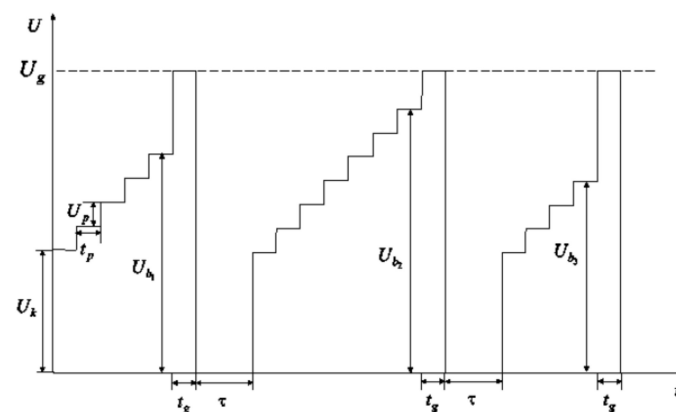


Figure 3. Process of breakdown voltage application: U_k —significantly smaller than the expected breakdown; U_g —value to which the voltage rises.

As can be seen in Figure 3, a fixed voltage U_k is applied to the gas component, which is significantly lower than the expected breakdown voltage U_b . Then, the voltage is increased by predetermined voltage steps U_p , whereby the duration of the voltage step t_p is set in advance. The ratio $k = U_p/t_p$ represents the voltage increase rate. When a breakdown occurs, the set value of the glow current i_g is provided by the voltage U_g during the glow time t_g , in order to establish a stationary concentration of charged and excited particles in the gas. The voltage at the electrodes of the gas component is then switched off during a time $\tau = 1$ s. When the set relaxation time expires, the process starts from the beginning. It should be pointed out that in order to determine the breakdown voltage U_b as accurately as possible, it is necessary to maintain constant parameters, such as voltage step U_p , the time between the two voltage stages t_p , the glow current $i_g = 0.5$ mA, the glow time $t_g = 1$ s and the relaxation time τ . This time τ is the period from the moment of interruption of voltage until reconnection of the voltage U_k . In this experiment, the voltage step was fixed at 0.1 V, while the duration of the steps varied from 0.01 s up to 0.1 s.

When the measurements of the breakdown voltage were taken, in a series of experiments repeated under the same conditions, the obtained breakdown voltage values were different. Since the breakdown voltage U_b has a statistical nature, because of a more accurate statistical analysis of the obtained data, it is necessary to perform a large number of measurements and to determine the mean value \bar{U}_b . In one series of this experiment, one thousand breakdown voltage measurements were performed for every value of the voltage increase rate. The same procedure was repeated for all components under the influence of radium gamma irradiation.

For most gas components, both those operating in the non-self-sustaining area and those operating in the breakdown voltage area (Geiger–Müller counters, surge arresters), it is necessary to know the minimum voltage that can be connected to the gas component when a breakdown occurs. This voltage value is called the static breakdown voltage U_s and is less than the value of U_b if the voltage increase rates are higher than 1 V/s. Based on the expression for the breakdown voltage probability, the static breakdown voltage can be defined as the maximum operating voltage U_w for which the probability of an electric breakdown is equal to zero, i.e., $\lim_{P \rightarrow 0} U_w = U_s$.

The static breakdown voltage U_s is a uniquely determined quantity, which could be estimated based on the measurements of various parameters. Although there are several methods for U_s estimation, the \bar{U}_b dependence on the voltage increase rate k was used in this research. In this paper, the value of the static breakdown voltage U_s is estimated as the intersection of the curve obtained by linear fitting of the experimental results $\bar{U}_b = f(k)$ and the y -axis, which corresponds to the value of $k = 0$. This could be expressed as $\lim_{k \rightarrow 0} \bar{U}_b = U_s$.

The static DC breakdown, on the other hand, occurs when the breakdown voltage is constant, and it is the static breakdown voltage U_s . For many gas-filled devices, determining their value is critical. Because of the statistical character of the breakdown process, a breakdown cannot occur quickly when voltage is provided to the gas component. The estimation of U_s breakdown voltage is most often performed in conditions of stepwise increase in voltage at the electrodes of the gas component, which represents the discretized dynamic method [32]. This method enables a more precise breakdown voltage determination than that by linear voltage raise [33]. The static breakdown voltage for the used components was estimated using the described method, and the results are shown in Figure 4. The estimated values of the static breakdown voltage for CITEL GFSA when not exposed to radiation and in the presence of gamma radiation were 227.3 V and 223 V, respectively. Likewise, the estimated values of the static breakdown voltage for Littelfuse GFSA were 264.4 V and 261.5 V when not exposed to radiation and in the presence of gamma radiation, while the values for the EPCOS GFSA were 289.9 V and 288.9 V without and with the presence of gamma radiation with the Ra source.

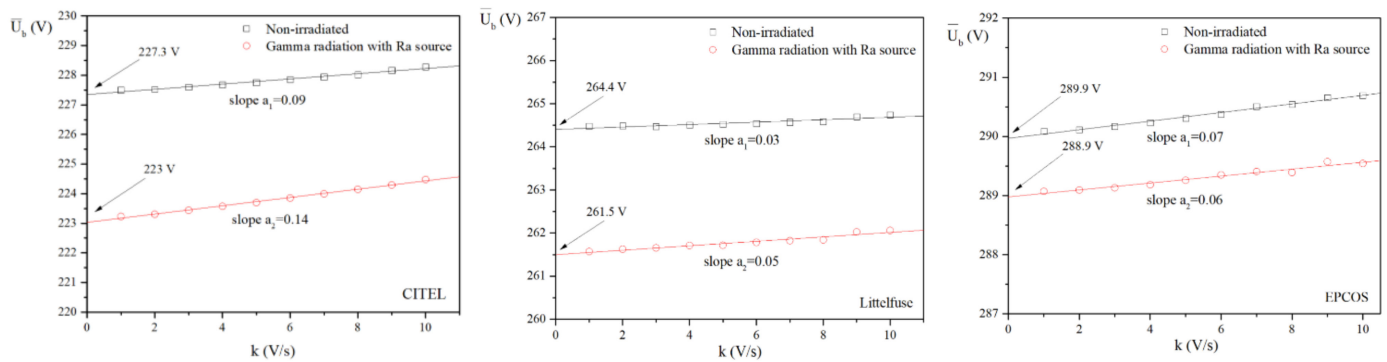


Figure 4. Mean value of breakdown voltage as a function of voltage increase rate for non-irradiated and gamma radiation with Ra source of CITEL, Littelfuse and EPCOS GFSAs, respectively.

The obtained results indicate that in the presence of gamma radiation originating from the Ra source, the value of the dynamic voltage decreases, as well as the estimated value of static breakdown voltage, which in this case is lower by 4.3 V for the irradiated CITEL GFSAs, also lower by 2.9 V for Littelfuse and lower by only 1 V for EPCOS (Figure 4). It was also calculated on the basis of the obtained data that the slope of the linear fit is lower when the radiation is not presented for CITEL and Littelfuse ($a_1 < a_2$) but almost equal for EPCOS ($a_1 \approx a_2$). It can be concluded from the obtained results that EPCOS GFSAs show the highest breakdown voltage stability. However, even though the other two arresters are about 4 and 3 V compared to the values from Table 1, these are prescribed deviations.

3. Results and Discussion

3.1. Statistical Analysis of Breakdown Voltage

Electrical breakdown characterization can be performed using three important variables: electrical breakdown probability, breakdown voltage and electrical breakdown delay time. The electrical breakdown in gas can be static or dynamic, depending on the type of applied voltage on the component. When the rate of voltage change is equal to or greater than the velocity of the elementary processes during the gas breakdown, the breakdown is dynamic and is defined by the dynamic breakdown voltage U_b . Due to the statistical nature of these processes, the breakdown does not occur at the same voltage value as the electrodes of the gas component. This means that the breakdown voltage takes place with a certain probability P . The voltage at which the transition from non-self-sustaining to self-sustaining discharge occurs is called the dynamic breakdown voltage U_b . Bearing in mind the statistical nature of the processes that lead to electrical breakdown in gas, and the gas components that we study operate on this principle, the investigation of the influence of radiation was also studied using various statistical methods. First of all, the influence of voltage increase rate and the impact of gamma radiation on the frequency count of dynamic breakdown voltage are shown in Figure 5. The results shown refer to the gas arrester manufactured by CITEL for a voltage increase rate of 1 to 3 V/s.

What the obtained results indicate is the following. Namely, with the growth in the voltage increase rate for these three values, there is no significant change in the width of the range of the measured values of the breakdown voltage. The exception occurs under the influence of radiation. The width of the interval of the measured values increases in the presence of radiation, i.e., approximately 3 V and 5.5 V without and in the presence of radiation, respectively. However, a shift of values toward higher values is observed, with the voltage increase rate's growth, while the radiation distribution shifts to the left toward lower values. A greater dispersion under the influence of radiation is observed, as well as a greater grouping of data in an interval close to the maximum value.

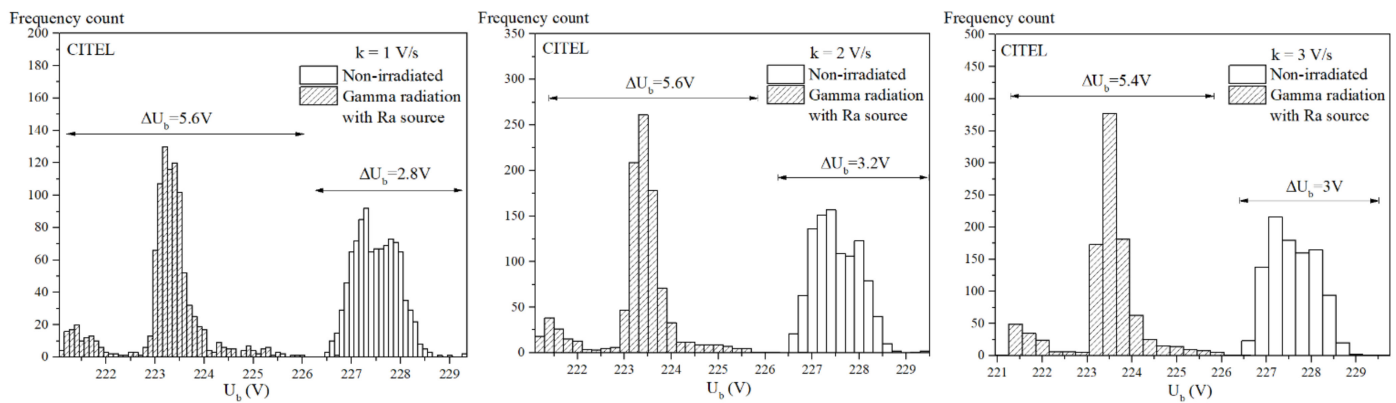


Figure 5. Frequency count of dynamic breakdown voltage of CITELE GFSAs for increase voltage rates $k = 1 \text{ V/s}$, $k = 2 \text{ V/s}$ and $k = 3 \text{ V/s}$ for non-irradiated arresters and ones in the presence of gamma radiation.

Figure 6 shows the frequency count distributions of breakdown voltage for three different manufacturers GFSAs at the same increase voltage rate of 1 V/s with and without the presence of radiation. It should be emphasized that the experiments were performed under the same conditions; each set of the measured values contained a thousand data, and the same dose of gamma radiation was presented. Similar behavior was noted in all cases. Such a tendency to increase the interval of the measured U_b values in the case where the component is irradiated was observed for all the other voltage increase rates, as can be seen in Figure 7. Under the influence of radiation, the obtained values of U_b decreased slightly, except for the EPCOS GFSAs, where an overlapping interval was observed, thus indicating the breakdown voltage stability. The observed dispersion of the measured values is greater in the presence of radiation, and there is also a greater number of sub-data in the interval around the maximum value. In Figure 6, the size of the scattering in each of the six cases is marked. The results we obtained for all ten increase voltage rates indicate a similar behavior, with the measured voltage values increasing with k for non-irradiated and irradiated gas-filled surge arresters.

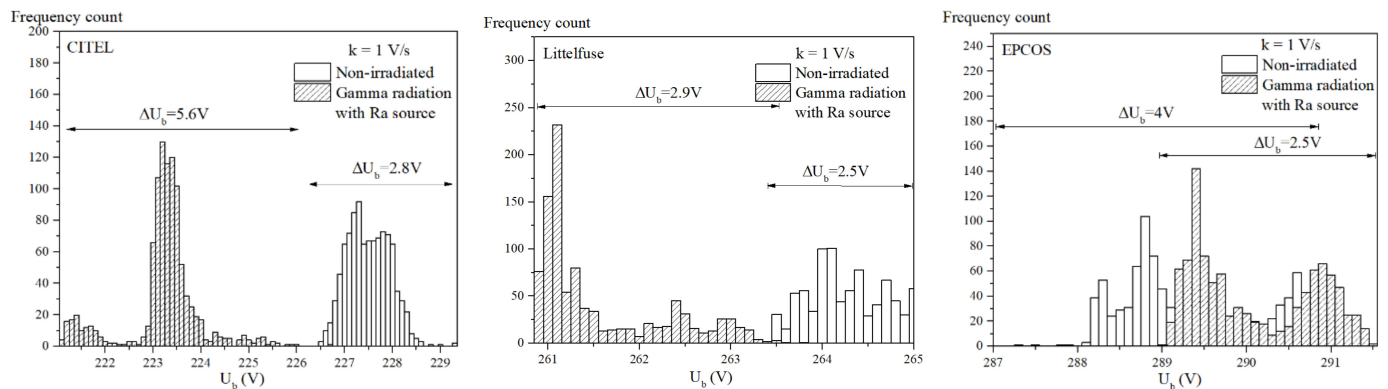


Figure 6. Frequency count of dynamic breakdown voltage of CITELE, Littelfuse and EPCOS GFSAs for increase voltage rate $k = 1 \text{ V/s}$ for non-irradiated arresters and ones in the presence of gamma radiation.

For a better insight into the results related to the irradiated components, Figure 7 shows the basic statistical values that describe one set of data for all ten voltage increase rates for all irradiated components. The results clearly confirm the stochastic nature of the breakdown voltages for voltage increase rates from 1 V/s to 10 V/s . This test was previously performed with other types of gas components that were not irradiated [34]. The standard deviation, mean value, median, maximum, minimum and 99 percentiles

represent all the main statistical characteristics of one analyzed variable. It can be noticed that the measured values for all components have a similar behavior, and good values are obtained without a large result scattering. This confirmed the reliability of the existence of thousands of measured data for each increase voltage rate used in further statistical analysis.

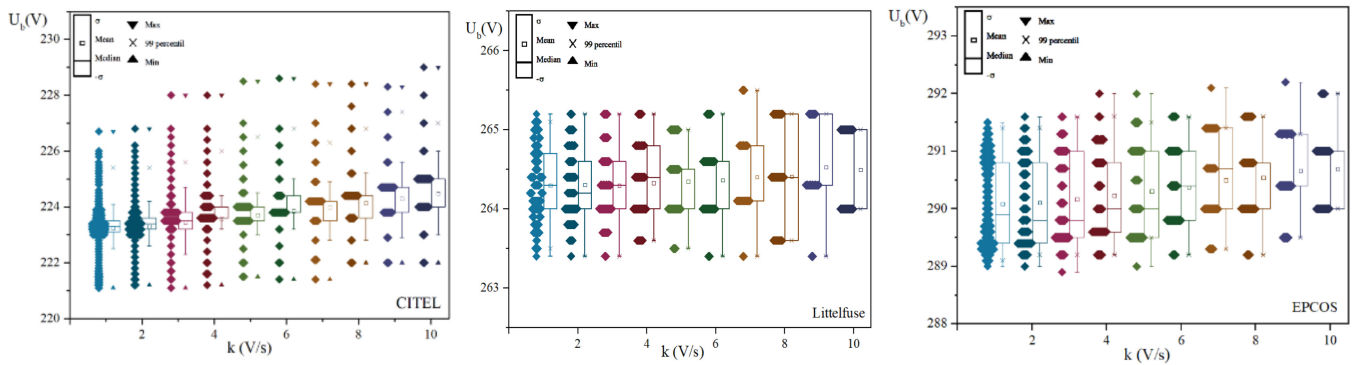


Figure 7. Standard deviation, mean, median, maximum, minimum and 99 percentiles of measurement results in the presence of gamma radiation for CITEL, Littelfuse and EPCOS GFSAs, respectively, for all voltage increase rates.

3.2. The Weibull Distribution and Parameters Estimation

As part of the results presented in this chapter have been published [1] and refer to the CITEL GFSAs, additional experiments and statistical data analysis for the same gas-filled surge arrester in the presence of gamma radiation were performed for a comparative analysis of their characteristics and reliability, together with Littelfuse and EPCOS GFSAs. In order to process the measured data, a cumulative distribution was performed for showing the probability of the variable to take a value less than or equal to a specific value. According to previous results and analyses [31,34] of the statistical behavior of the electric breakdown voltage distribution of a xenon-filled tube, the Weibull function presented a good agreement between the theory and the experiment, so it was performed in this case as well. Namely, the Weibull distribution was chosen as it is often used for performing the life data analysis—calculating the lifetime characteristics. The reliability of the GFSAs used in this article could be determined by using this method. The research results can provide data, which could be used in future performance of GFSAs.

The Weibull distribution is used for evaluating the reliability and material strengths of many different fields, including vacuum tubes and capacitors, as well as relays and ball bearings. Aside from that, it can also model hazard decreasing, increasing or constant functions, so it allows describing any phase of an item’s lifetime [35]. With the appropriate parameters and with the lifetime characteristics, through the Weibull distribution, the experimental values of the lifetime can be determined [36].

Weibull models are used to describe various types of observed failures of components and phenomena [35]. Additionally, they are widely used in reliability and survival analysis in this paper. The following formula for distribution of experimental data of the dynamic breakdown voltage is used [37,38]:

$$F(U_b) = 1 - \exp\left(-\left(B * (U_b - U_a)\right)^d\right) \tag{1}$$

In Formula (1), the first parameter B is the characteristic life of the component, known as the scale parameter. There is also U_a , known as the failure free life or the location parameter, and last but not least, the shape parameter d , or the slope. Thus, the three-

parameter Weibull distribution in the formula, showing the unreliability of the component, is $F(U_b)$. With it, the reliability of the component $R(U_b)$ can also be defined as

$$R(U_b) = \exp\left(- (B * (U_b - U_a))^d\right). \tag{2}$$

From the formula and the presented results, it should be noted that the most important parameter for behavior estimation of the breakdown voltage is parameter d .

In order to verify the influence of gamma radiation on the distribution of experimental dynamic breakdown voltage data, their fitting was performed using Equation (1). As we have less data scattering with a growth of the increase voltage rate, the continuation of the validation test of the Weibull function distribution was presented for the first three. Because of that, in Figures 8 and 9, the cumulative distributions for both cases are given for voltage increase rates $k = 1 \text{ V/s}$ to 3 V/s . The histograms in Figure 8 (non-irradiated) and Figure 9 (gamma radiation with Ra source) show the experimental distribution functions, whereas the solid red lines represent the Weibull distribution fits.

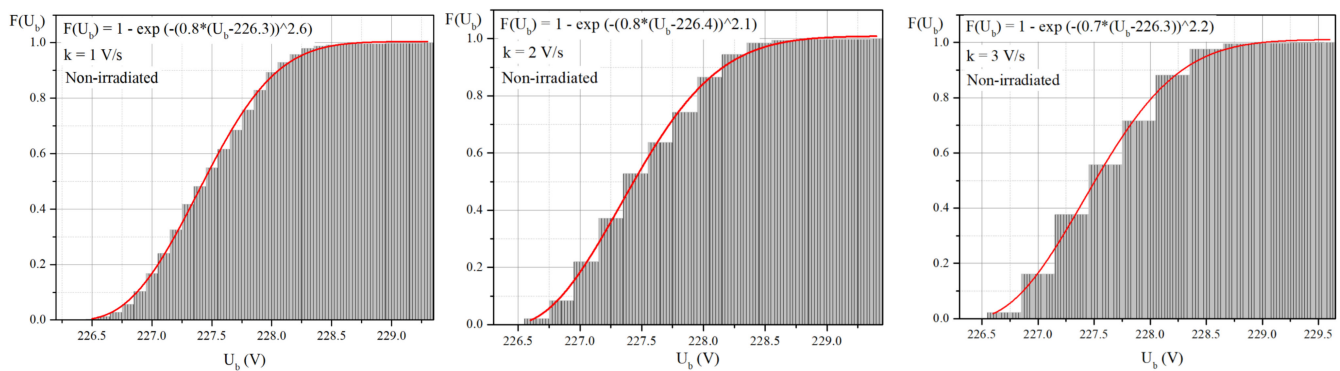


Figure 8. Cumulative distribution functions of non-irradiated CITELE GFSAs for increase voltage rates $k = 1 \text{ V/s}$, $k = 2 \text{ V/s}$, and $k = 3 \text{ V/s}$, respectively.

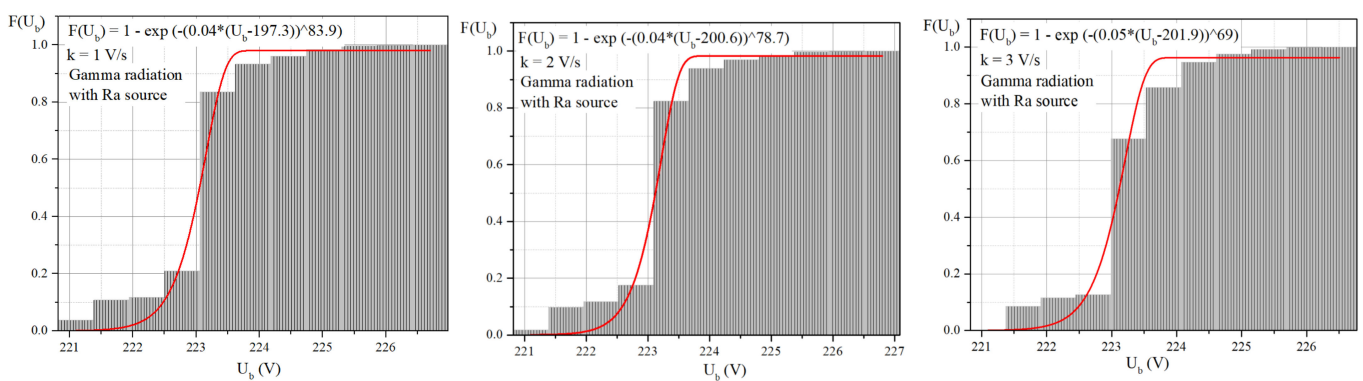


Figure 9. Cumulative distribution functions of CITELE GFSAs in the presence of gamma radiation for increase voltage rates $k = 1 \text{ V/s}$, $k = 2 \text{ V/s}$, and $k = 3 \text{ V/s}$, respectively.

As this paper is an extended version of the publication [1], the research related to CITELE GFSAs is presented in more detail. The results for all ten voltage increase rates were examined, but only the first three are shown. Table 2 shows the estimated values of the parameters of the Weibull distribution obtained by fitting the experimental results, as well as the values of the correlation coefficient R^2 , as well as the results of the non-parametric Pearson χ^2 test. The results show slightly better agreement of the Weibull distribution with the experimental data when the arrester was not irradiated.

Table 2. Weibull distribution parameters, R^2 and χ^2 coefficients for CITELE GFSAs without and in the presence of gamma radiation.

k (V/s)	B		U_a		d		R^2		χ^2	
	Non-Irradiated	Irradiated								
1	0.8	0.04	226.3	197.3	2.6	8.3	0.996	0.882	0.00016	0.00320
2	0.7	0.04	226.4	200.6	2.1	8.7	0.995	0.991	0.00079	0.00295
3	0.7	0.05	224.3	201.9	2.9	6.9	0.988	0.855	0.00157	0.00438

The performed fitting procedure led to different values of Weibull distribution parameters. For these reasons, the distribution parameters themselves were individually analyzed for all ten increase voltage rates. As can be seen in Table 2, the value of parameter U_a obtained is very close to the previously estimated value of the static breakdown voltages of CITELE GFSAs using the dynamic discretized method and confirms the possibility of estimating the value of static breakdown voltage in this way and with the need to indicate that it is possible with an adequate number of performed breakdown voltage measurements for every k .

The experimental distribution functions of breakdown voltage for voltage increase rate of 1 V/s are shown in Figure 10. These results were obtained for non-irradiated CITELE, Littelfuse and EPCOS GFSAs, respectively. The experimental distribution functions are shown with histograms (without bar). All the measured values and corresponding frequencies are used for drawing the experimental distribution functions. The experimental distribution functions are fitted with the Weibull distributions' function given by Equation (1). This Weibull fits are presented in Figure 10 with red lines.

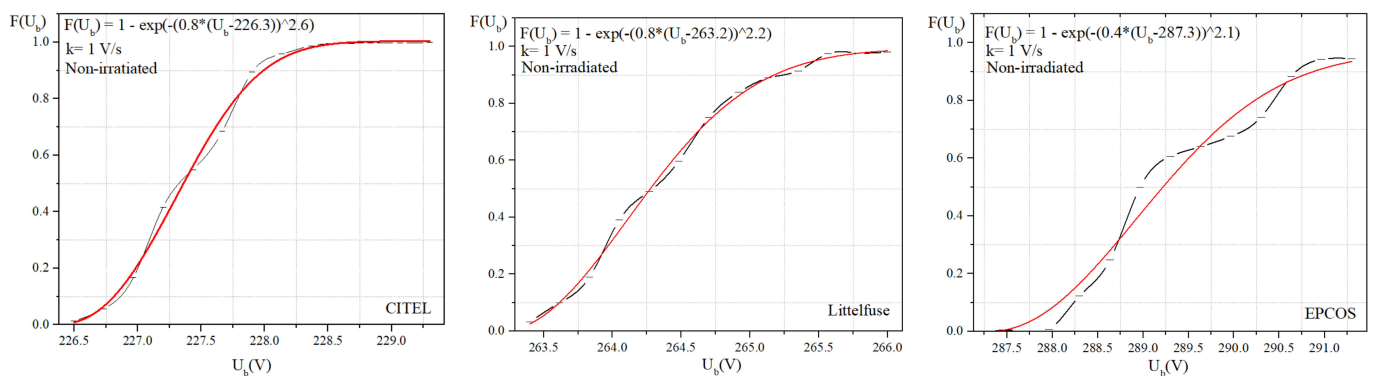


Figure 10. Cumulative distribution functions of non-irradiated CITELE, Littelfuse and EPCOS GFSAs, respectively, for increase voltage rates $k = 1$ V/s.

Figure 11 shows the experimental distribution function of breakdown voltage obtained in the presence of gamma radiation for CITELE, Littelfuse and EPCOS GFSAs, respectively. The presented results were obtained experimentally for the voltage increase rate of 1 V/s. The experimental distribution functions are shown with histograms (without bar). The experimental cumulative distributions were fitted with the Weibull distributions' function (marked as a red line in the figures), which is given by Equation (1).

Table 3 shows the parameters of the Weibull distribution obtained by fitting the experimental results without and in the presence of gamma radiation. In addition, the value of the correlation coefficient was given, which in the case of non-irradiated and irradiated components was closer to unity, thus confirming the good agreement between the theoretical setting and the experimental results in this case for all types of gas arresters used in the experiments. The results of the non-parametric Pearson χ^2 test were also considered.

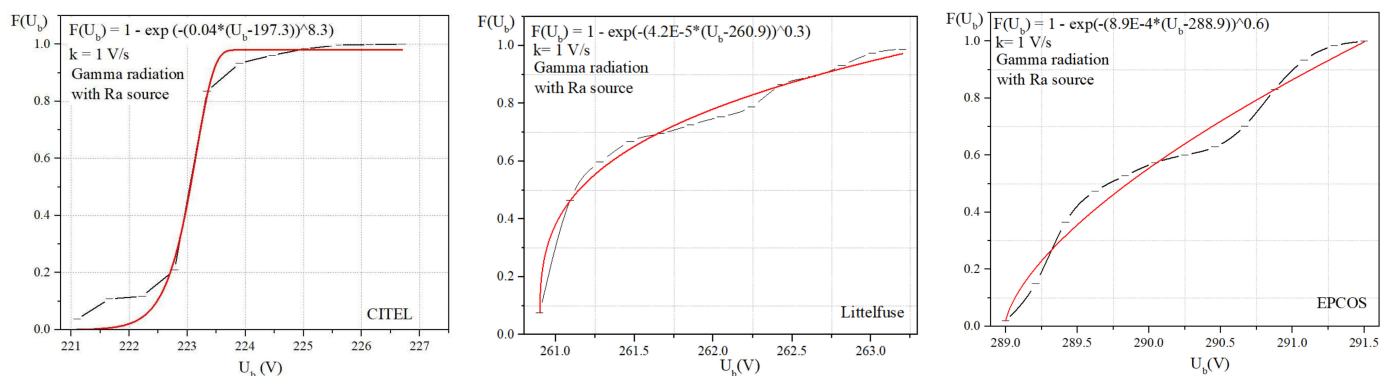


Figure 11. Cumulative distribution functions of CITEL, Littelfuse and EPCOS GFSAs, respectively, in the presence of gamma radiation for increase voltage rates $k = 1 \text{ V/s}$.

Table 3. Weibull distribution parameters, R^2 and χ^2 coefficients for CITEL, Littelfuse and EPCOS GFSAs without and in the presence of gamma radiation.

$k = 1 \text{ V/s}$ Component	B		U_a		d		R^2		χ^2	
	Non-Irradiated	Irradiated	Non-Irradiated	Irradiated	Non-Irradiated	Irradiated	Non-Irradiated	Irradiated	Non-Irradiated	Irradiated
CITEL	0.8	0.04	226.3	197.3	2.6	8.3	0.996	0.882	0.00023	0.00320
Littelfuse	0.8	4.2×10^{-5}	223.2	260.9	2.2	0.3	0.997	0.992	0.00036	0.00196
EPCOS	0.4	8.9×10^{-4}	287.3	288.9	2.1	0.6	0.979	0.976	0.00152	0.00318

Another important acquired value is the coefficient of correlation R^2 [34], as it shows the relationship strength between the Weibull distribution fit and the experimental distribution functions. In this article, all values from all graphs are $R^2 > 0.88$, which demonstrates that the value is very close to 1, showing that the model fits the observed data very well. This conclusion is valid for all types of GFSAs used in the non-irradiated experiments and those in the presence of gamma radiation. This fact indicates that the suggested Weibull distribution could be used for the breakdown voltage distribution function for CITEL, Littelfuse and EPCOS GFSAs with and without additional gamma radiation. The results of the analysis are shown in Tables 1 and 2. In addition, the values of the non-parametric Pearson χ^2 test are shown.

Interestingly, reproducibility was also observed in the irradiated GFSAs samples of all mentioned manufacturers, in contrast to our previous experiments with xenon-filled gas tubes [31], where the sample used did not show a good agreement with the Weibull distribution to such an extent. Namely, during the analysis of experimental results for different voltage increase rates, the values for R^2 went up to 0.758 in the presence of radiation, which indicates the reliability of GFSAs under different experimental conditions.

4. Conclusions

The paper presents the results of the reliability testing of gas-filled surge arresters manufactured by CITEL, Littelfuse and EPCOS at the same operating voltage of 230 V, with and without the presence of gamma radiation of the radium source. As the breakdown voltage has a stochastic nature, one thousand measurements of breakdown voltage under the same experimental conditions were performed in all experiments. The values of glow current, glow time, relaxation and the same initial voltage value were performed for each voltage increase rate k from 1 V/s to 10 V/s. The dependence of $\bar{U}_b = f(k)$, where the mean value of U_b is obtained on the basis of one thousand voltage measurements, was presented. The value of the static breakdown voltage in the case when the component was non-irradiated and in the presence of gamma radiation was estimated by the dynamic

method using linear fit, and the values were 227.3 V and 223 V, 264.4 V and 261.5 V, 289.9 V and 288.9 V, for CITEL, Littelfuse and EPCOS GFSAs, respectively. It is concluded that there is a slight decrease in the value of the static breakdown voltage due to irradiation, which indicates the stability of the breakdown voltage of these components.

The frequency count distributions of U_b were shown for CITEL GFSAs for three voltage increase rates without and with additional gamma radiation. Moreover, similar comparison was performed for all three GFSAs used in the experiments for $k = 1$ V/s. Two important conclusions could be drawn. The range of the measured U_b values at certain voltage increase rate grows under the influence of gamma radiation. Further, such a tendency to increase the interval of the measured U_b values in the case when the component is irradiated was observed for all the other voltage increase rates. It could be emphasized that in the presence of gamma radiation, the most experimental values grouped in an interval close to the maximum value. In order to have a better insight into the distribution of the measured breakdown voltage values in the presence of radiation for all three components for all ten voltage rise rates, basic statistical variables were calculated, such as the standard deviation, mean value, median, maximum, minimum and 99 percentiles, and their graphical presentations were given. It was found that one thousand data were enough for reliability assessment and further analysis in all cases.

Due to the importance and large application of the Weibull distribution, it was used for fitting the cumulative distribution functions for non-irradiated component as well as in the presence of gamma radiation, and that procedure exhibited a good agreement between the theory and the experimental data. Since the Weibull distribution parameters were not the same for all GFSAs, all their values were shown. It was found that the values of U_a and d in the sum gave the mean value of the breakdown voltage obtained experimentally. Additionally, parameter U_a confirms that their values are close to the U_s values obtained by the dynamic method. The good choice of the function for fitting the data was confirmed by the coefficient of correlation, which was approximately close to 1, as well as Pearson χ^2 -test in all cases with and without radiation for all types of GFSAs.

It is important to note that this research may have significant engineering implications related to the safety and failure mode for demanding applications of surge protection industry associated with military installations that may be exposed to nuclear electromagnetic pulses [39,40]. It can also be seen in general that the performance of CITEL, Littelfuse and EPCOS GFSAs under gamma radiation makes it suitable for overvoltage protection of electronic circuitry constantly or occasionally exposed to that type of radiation. Because of that, our further research will be based on the reliability analysis of gas-filled arresters testing the response time of this component using the time delay method, as well as the effect of radiation on it, which will be an essential concept in our further experiments.

Author Contributions: Conceptualization, E.Ž.; methodology, E.Ž.; experiment, M.Ž. and S.V.; formal analysis, E.Ž., M.Ž. and S.V.; investigation, E.Ž.; M.Ž. and S.V.; writing—original draft preparation, E.Ž.; M.Ž. and S.V. All authors have read and agreed to the published version of the manuscript.

Funding: This research was funded by Ministry of Education, Science and Technological Development of Republic of Serbia. Program for financing scientific research work (grants no. 451-03-68/2022-14/200102).

Data Availability Statement: Initial results was published in Proceedings of the 32nd International Conference on Microelectronics, Niš, Serbia, 12–14 September 2021.

Acknowledgments: The work is supported by Ministry of Education, Science and Technological Development of Republic of Serbia. Program for financing scientific research work (grants no. 451-03-68/2022-14/200102). This research was funded by the European Union's Horizon 2020 research and innovation program under grant agreement No. 857558.

Conflicts of Interest: The authors declare no conflict of interest.

References

1. Živković, M.; Dimitrijević, N.; Živanović, E. Statistical Analysis of Breakdown Voltage of Citel Gas-filled Surge Arrester. In Proceedings of the 32nd International Conference on Microelectronics, Niš, Serbia, 12–14 September 2021; pp. 113–116.
2. Pejović, M.M. *Introduction to Electrical Gas Discharges. Gas Electronic Components, Chapter 8*; University of Niš, Faculty of Electronic Engineering: Niš, Serbia, 2008; pp. 124–128.
3. Pham, C.D.; Crevenat, V.; Gannac, Y. Empirical model of the impulse voltage-time characteristic of gas discharge tube. In Proceedings of the 35th International Conference on Lightning Protection, Colombo, Sri Lanka, 20–26 September 2021.
4. Gannac, Y.; Leduc, G.; Pham, C.-D.; Crevenat, V. 8/20 and 10/350 surges behaviour of a gas discharge tube according to gas pressure. *Electr. Pow. Syst. Res.* **2021**, *197*, 107302. [CrossRef]
5. Huttner, L.; Jurcacko, L.; Valent, F.; Ehrhardt, A.; Schreiter, S.; Rock, M. Basic problems and solution of the encapsulation of a low-voltage spark gap with arc splitter chamber. *J. Electric. Eng.* **2012**, *63*, 103–108. [CrossRef]
6. Finis, G.; Wetter, M.; Meyer, T. New spark-gap technology with efficient line-follow current suppression for the protection of powerful LV distribution systems. In Proceedings of the 33rd International Conference on Lightning Protection, Estoril, Portugal, 25–30 September 2016.
7. Rozman, R. Gas Discharge Tube Assemblies. U.S. Patent 2020/0161073 A1, 12 May 2020.
8. Tsovilis, T.E. Critical insight into performance requirements and test methods for surge protective devices connected to low-voltage power systems. *IEEE Trans. Pow. Del.* **2021**, *36*, 3055–3064. [CrossRef]
9. Arbutina, D.S.; Vasić-Milovanović, A.I.; Nedić, T.M.; Janičević, A.J.; Timotijević, L.B. Possibility of Achieving an Acceptable Response Rate of Gas-Filled Surge Arresters by Substitution of Alpha Radiation Sources by Selection of Electrode Material and the Electrode Surface Topography. *Nucl. Technol. Radiat. Prot.* **2020**, *35*, 223–234. [CrossRef]
10. Osmokrović, P.; Vasić, A.; Živić, T. The Influence of the Electric Field Shape on the Gas Breakdown Under Low Pressure and Small Inter-Electrode Gap Conditions. *IEEE Transactions on Plasma Science* **2005**, *33*, 1677–1681. [CrossRef]
11. Osmokrović, P.; Živić, T.; Lončar, B.; Vasić, A. The Validity of the General Similarity Law for Electrical Break down of Gases. *Plasma Sources Sci. Technol.* **2006**, *15*, 703–713. [CrossRef]
12. Stanković, K.; Alimpijević, M. Free-Electron Gas Spectrum Uniqueness in the Mixture of Noble Gases. *Contrib. Plasma Phys.* **2016**, *56*, 126–133. [CrossRef]
13. Pejović, M.M.; Nešić, N.T.; Pejović, M.M.; Brajović, D.V.; Denić, I.V. Investigation of Post-Discharge Processes in Nitrogen at Low Pressure. *Phys. Plasmas* **2012**, *19*, 123512. [CrossRef]
14. Živanović, E. Influence of combined gas and vacuum breakdown mechanisms on memory effect in nitrogen. *Vacuum* **2014**, *107*, 62–67. [CrossRef]
15. Lucchini, F.; Marconato, N.; Bettini, P. Automatic Optimization of Gas Insulated Components Based on the Streamer Inception Criterion. *Electronics* **2021**, *10*, 2280. [CrossRef]
16. Deng, S.; Morrison, A.P.; Guo, Y.; Teng, C.; Chen, M.; Cheng, Y.; Liu, H.; Xiong, X.; Yuan, L. Design of a Real-Time Breakdown Voltage and On-Chip Temperature Monitoring System for Single Photon Avalanche Diodes. *Electronics* **2021**, *10*, 25. [CrossRef]
17. Vavilov, V.S.; Ukhin, H.A. *Radiation Effects in Semiconductors and Semiconductors Devices*, 1st ed.; Consultants Bureau: New York, NY, USA, 1977.
18. Stojadinović, N.; Djorić-Veljković, S.; Davidović, V.; Golubović, S.; Stanković, S.; Prijić, A.; Prijić, Z.; Manić, I.; Danković, D. NBTI and irradiation related degradation mechanisms in power VDMOS transistors. *Microelectron. Reliability* **2018**, *88–90*, 135–141. [CrossRef]
19. Djorić-Veljković, S.; Manić, I.; Davidović, V.; Danković, D.; Golubović, S.; Stojadinović, N. Annealing of Radiation-Induced Defects in Burn-in Stressed Power VDMOSFETs. *Nucl. Technol. Radiat. Prot.* **2011**, *26*, 18–24. [CrossRef]
20. Martínez, P.J.; Maset, E.; Martín-Holgado, P.; Morilla, Y.; Gilabert, D.; Sanchis-Kilders, E. Impact of Gamma Radiation on Dynamic RDSON Characteristics in AlGaN/GaN Power HEMTs. *Materials* **2019**, *12*, 2760. [CrossRef] [PubMed]
21. Rubinjoni, L.; Karadžić, K.; Lončar, B. Influence of Gamma Radiation on Gas-Filled Surge Arresters. In *Use of Gamma Radiation Techniques in Peaceful Applications*; Chapter 13; Almayah, B.A., Ed.; IntechOpen: London, UK, 2019.
22. Živanović, E.; Veljković, S.; Živković, M.; Pejović, M. Reliability of various type of gas-filled surge arresters under DC discharge. In Proceedings of the 31st International Conference on Microelectronics, Niš, Serbia, 16–18 September 2019; pp. 113–116.
23. Živanović, E.; Živković, M.; Pejović, M. The Evolution of Breakdown Voltage and Delay Time Under High Overvoltage for Different Types of Surge Arresters. *Facta Univ. Ser. Electron. Energetics* **2021**, *34*, 307–322. [CrossRef]
24. Pejović, M.M.; Pejović, M.M. Investigation of breakdown voltage and time delay of gas-filled surge arresters. *J. Phys. D Appl. Phys.* **2006**, *39*, 4417–4422. [CrossRef]
25. Lončar, B.; Vujisić, M.; Stanković, K.; Arandić, D.; Osmokrović, P. Radioactive Resistance of Some Commercial Gas Filled Surge Arresters. In Proceedings of the 26th International Conference on Microelectronics, Niš, Serbia, 11–14 May 2008; pp. 587–590.
26. CITELE Surge Protection. Available online: <https://citel.fr/en/gdt/2-electrode> (accessed on 6 July 2022).
27. Littelfuse Surge Protection. Available online: <https://www.littelfuse.com/media?resourcetype=datasheets&itemid=e3c9bc9e-6b2c-4bc9-92b2-d903d0925a22&filename=littelfuse-gdt-ac-cg3-datasheet> (accessed on 6 July 2022).
28. EPCOS Surge Protection. Available online: <https://docs.rs-online.com/c5e1/A700000008614351.pdf> (accessed on 6 July 2022).
29. Ropp, R.C. The Alkaline Earths as Metals. In *Encyclopedia of the Alkaline Earth Compounds*, 1st ed.; Elsevier: Amsterdam, The Netherlands, 2013; pp. 1–23.

30. Gad, S.C. Radium. In *Encyclopedia of Toxicology*, 3rd ed.; Elsevier: Amsterdam, The Netherlands, 2014; pp. 44–45.
31. Pejović, M.; Živanović, E.; Stojanović, M. Xenon-filled diode performance under influence of low doses of gamma radiation. *Appl. Radiat. Isot.* **2022**, *184*, 110207. [[CrossRef](#)]
32. Pejović, M.M. Digital system for vacuum and gas-filled devices testing. *Rev. Sci. Instrum.* **2005**, *76*, 015102. [[CrossRef](#)]
33. Pejović, M.M.; Milosavljević, Č.S.; Pejović, M.M. The estimation of static breakdown voltage for gas-filled tubes at low pressures using dynamic method. *IEEE Trans. Plasma Sci.* **2003**, *31*, 776–781. [[CrossRef](#)]
34. Živanović, E.; Maluckov, Č. Investigation of statistical behaviour of electrical breakdown voltage distribution for nitrogen-filled diode at 13.3 mbar pressure. *Contrib. Plasma Phys.* **2018**, *58*, 293–301. [[CrossRef](#)]
35. Müller, P.H.; Neumann, P.; Storm, R. *Tafeln der Mathematischen Statistik*; VEB Fachbuchverlag: Leipzig, Germany, 1973.
36. Lai, C.-D.; Pra Murthy, D.N.; Xie, M. *Weibull Distributions and Their Applications*; Chapter 2, Springer Handbook of Engineering Statistics; Pham, H., Ed.; Springer: Berlin/Heidelberg, Germany, 2006; pp. 63–78.
37. Weibull, W. A statistical distribution function of wide applicability. *J. Appl. Mech.* **1951**, *18*, 293–297. [[CrossRef](#)]
38. Larsen, R.J.; Marx, M.L. *An Introduction to Mathematical Statistics and Its Applications*, 5th ed.; Pearson Education, Inc.: London, UK, 2012; pp. 221–280.
39. Electromagnetic Pulse (EMP) Protection and Resilience Guidelines for Critical Infrastructure and Equipment, National Coordinating Center for Communications (NCC), Unclassified, National Cybersecurity and Communications Integration Center Arlington, 2019, Virginia, USA. pp. 1–133. Available online: <https://michaelmabee.info/electromagnetic-pulse-emp-protection-and-resilience-guidelines/> (accessed on 6 July 2022).
40. Tsovilis, T.E.; Topcagic, Z. DC overload behavior of low-voltage varistor-based surge protective devices. *IEEE Trans. Power Deliv.* **2020**, *35*, 2541–2543. [[CrossRef](#)]